A NEW PCA–BASED ROBUST COLOR IMAGE WATERMARKING METHOD

Arash Abadpour and Shohreh Kasaei

Sharif University of Technology, Tehran, Iran

ABSTRACT

Although, the possibility of electronic storage and transmission has been beneficial for extending the intellectual communication, the easiness of copying and transmitting the data in the internet has increased the piracy and illegal use of owned artworks. As a result, digital data watermarking, has been under thorough investigation in recent years. The main aim of data hiding is to add some transparent signature to the data in an attack–resistance fashion, to be used for ownership claims. In this paper a new PCA–based watermarking method is proposed for color images. Rather than the dominant spatial, and the few available semi–spectral approaches, the proposed method uses the true redundancy in the spectral domain. The proposed watermarking method is resistent to available attacks, such as sophisticated geometrical transformations, artistic effects, lossy compression, frequency domain filtering, motion blur, occlusion, and enhancement. Experimental results show the efficiency of the proposed algorithm.

1. INTRODUCTION

The spread of the electronic data on the internet has emerged the need to take larger steps towards copyright protection. Thus, there has been a need to *watermark* the artworks for legal reasons since development of the multimedia systems and the cyberworld [1]. Digital watermarking is performing significantly preferable, when compared to the conventional *cryptography* systems, because it adds a transparent signature to the data. In this way, the artwork is not protected against being used by authorized users, but the ownership is preserved. Some authors work on methods for general–purpose digital data watermarking(*e.g.*, [2, 3]). These approaches do not use the problem–specific constraints and possibilities. Also, as watermarking has a very tight relation to cryptography, some researchers have tried to solve both problems at once (*e.g.*, see [2, 4]). Here, we draw a line between these two different approaches of finding some empty places in the image for embedding some data, and to encrypt that data. The main concern of data hiding, is to find those portions of the image domain that are ignored by the human observer. Since the birth of the watermarking concept, many researchers have worked on the redundancy of natural images in the spatial domain, resulting in high performance spatial watermarking techniques [1]. Although, some researchers have worked on data hiding using the spectral redundancy (*e.g.*, see [3]), but small work has been performed on finding the real redundant spectral data in the image. Generally, authors work on some subjectively–investigated assumption about the color channels [3, 5, 6]. For example in [3] the authors add the watermark to the *blue* plane. In [6] the author use the $CIE-Lab$ color space in a simple quantization method, to add the color watermark in the least significant bits. Many other authors have tried the quantization techniques [3, 4, 6], which shows itself as an additive noise, and its robustness when attacked with noise removal methods, is doubtful. In this paper, we address the special problem of color image watermarking using the perceptual gaps in natural images in the spectral domain, which could be filled with watermark data, without disturbing the visual appeal of the original image, using the eigenimage theory.

2. PROPOSED ALGORITHM

2.1. Reconstruction Error–Based Homogeneity Criteria

In [7], the authors proposed to use the error made by neglecting the two less important principal components as a likelihood measure. The likelihood of the vector $\vec{c}$ to the cluster r is defined as $e_r(\vec{c}) = \|\acute{\vec{v}}(\vec{c}-\vec{\eta})\vec{v}-(\vec{c}-\vec{\eta})\|$, where, $\vec{v}$ shows the direction of the first principal component and $\|\vec{x}\|$ denotes the normalized L_1 norm. In [7] the authors proposed to use the following stochastic norm as the region homogeneity: $\|f\|_{r,p} = arg_e(P_{\vec{x}\in r}\{f(\vec{x}) \leq e\} \geq p)$, where p is the inclusion percentage. The $\|e_r\|_{r,p}$ is proved to outperform conventional *Euclidean* and *Mahalanobis* approaches [8]. The criterion is used for *quad–tree decomposition* [9] as a rough image segmentation tool.

Arash Abadpour is with the Mathematics Science Department, Sharif University of Technology, Tehran, Iran, P.O. Box 11365-9517, email: abadpour@math.sharif.edu

Shohreh Kasaei is with Computer Engineering Department, Sharif University of Technology, Tehran, Iran, P.O. Box 11365-9517, email:skasaei@sharif.edu

2.2. Bi-tree Decomposition

Having a suitable homogeneity criteria, the image can be decomposed into homogenous blocks. Starting with the entire image area, the tree is produced using the homogeneity criteria defined as $\|e_r\|_{r,p} \leq \varepsilon_1$, where ε_1 is a user-selected parameter, mostly in the range $[1 \ldots 10]$. In an $W \times H$ image, the *depth* of a $w \times h$ block r is defined as $\varrho_r = \max\{\log_2 \frac{W}{w}, \log_2 \frac{H}{h}\}$ and no block is permitted to reach to the depth more than a preselected marginal depth value ϱ. During the decomposition stage, all the information is saved as a $22 \times N$ matrix called Λ, where N is the number of the blocks and each column of Λ consists of x_1, y_1, x_2, y_2, η_1, η_2, η_3, $V_{ij}, i, j = 1, \cdots, 3$ and some reserved parameters. Where, $[\eta_1, \eta_2, \eta_3]^T$ is the expectation of the color information and V_{ij} are the elements of the PCA Matrix V, both corresponding to the block r. Assume that the image I is fed to the *bi–tree* decomposition method. If the block r is not enough homogenous, rather than the deterministic choice of sub–blocks in the quad–tree decomposition method, here, two sets of alternatives for decomposition are proposed. Assume that splitting r to two equal rectangles vertically gives the two regions of r_1 and r'_1 while splitting horizontally results in r_2 and r'_2. Now, if $\|e_{r_1}\|_{r_1,p} + \|e_{r'_1}\|_{r'_1,p} < \|e_{r_2}\|_{r_2,p} + \|e_{r'_2}\|_{r'_2,p}$ and the depth limitation permits, the block is split vertically and otherwise (if the depth limitation is met) it is split horizontally. In the new method, the rectangular clipping is reserved while the block shape changes to best fit the image details.

2.3. Basis Vectors Polarization

Suppose the space R^n and a set of n basis vectors $\vec{v}_i, i = 1, \cdots, n$. Storing this set of vectors needs n^2 cells of memory, when neglecting the redundancy of the data. Having in mind that a set of basis vectors are an *ortho–normal* set, the actual needed memory can be reduced. In fact, a set of basis vectors of R^n is a member of R^{n^2}, with n constraints of normality ($\|\vec{v}_i\| = 1, i = 1, \cdots, n$) and $\frac{n(n-1)}{2}$ constraints of orthogonality ($\vec{v}_i \perp \vec{v}_j, i, j = 1, \cdots, n, i \neq j$). Thus, the above–mentioned set of basis vectors is an unconstrained member of an m dimensional space, with $m = n^2 - n - \frac{n(n-1)}{2} = \frac{n(n-1)}{2}$. Thus, storing a set of basis vectors of R^n in $\frac{n(n-1)}{2}$ memory cells contains zero redundancy. To make this representation unique, it is crucial to make the set of basis vectors *right–rotating* (RR). In 2–D spaces, RR means $(\vec{v}_1 \times \vec{v}_2) \cdot \vec{j} > 0$, where, $\times$ and $\cdot$ stand for the *outer* and the *inner* products, respectively. In 3–D spaces, RR means $(\vec{v}_1 \times \vec{v}_2) \cdot \vec{v}_3 > 0$. Setting $n = 2$ leads to $m = 1$, which means that any set of RR basis vectors in the xy plane can be specified uniquely by a single angle. Similarly, the case of $n = 3$ results in $m = 3$, which is used in this paper. Note that, in both cases the m parameters are angles between vectors and some fixed planes. Though, we call this method the *polarization* method. Consider the three right rotating vectors $\vec{v}_1, \vec{v}_2, \vec{v}_3$ in R^3, we define the three angles θ, ϕ, and ψ as follows. This representation is a manipulated version of the well–known set of *Euler* angles. Using $\vec{v}^p$ as the projection of $\vec{v}$ on the plane p (*e.g.* $\vec{v}_1^{xy}$), the three angles are defined as:

$$\begin{cases} \theta = \angle(\vec{v}_1^{xy}, [1,0]^T) \\ \phi = \angle((R_\theta^{xy} \vec{v}_1)^{xz}, [1,0]^T) \\ \psi = \angle((R_\phi^{xz} R_\theta^{xy} \vec{v}_2)^{yz}, [1,0]^T) \end{cases} \tag{1}$$

where, $\angle(\vec{v}, \vec{u})$ stands for the angle between the two vectors $\vec{v}, \vec{u} \in R^2$. Also, R_α^p is the 3×3 matrix of α radians counter–clock–wise rotation in the p plane. It can be easily proved, using 3–D geometrical concepts, that the 3×3 matrix V with $\vec{v}_i$ as its i–th column satisfies, $R_\psi^{yz} R_\phi^{xz} R_\theta^{xy} V = I$. Having in mind that, $(R_\alpha^p)^{-1} = R_{-\alpha}^p$, wa have $V = R_{-\theta}^{xy} R_{-\phi}^{xz} R_{-\psi}^{yz}$. While equation (1) computes the three angles θ, ϕ, and ψ out of the basis vectors (*polarization*), the above matrix multiplication, reproduces the basis from θ, ϕ, and ψ (*depolarization*).

2.4. Blockwise Interpolation

Assume a partition of $N_W \times N_H$ into the set of rectangular regions $\{r_i | i = 1, \cdots, n\}$, with corresponding values of $\{\lambda_i | i = 1, \cdots, n\}$, satisfying $\lambda_i = \arg_\lambda \left(\forall \vec{c} \in r_i, f(\vec{c}) \simeq \lambda\right)$, for an unknown smooth function $f : R^2 \to R$. The problem is to find $\tilde{f}$ as an approximation of f using r_i and λ_i. We address this problem as *blockwise interpolation* of the set $\{(r_i; \lambda_i) | i = 1, \cdots, n\}$. Note that in the case that the partition is a rectangular grid, the problem reduces to an ordinary 2–D interpolation task. Here, we use the same idea with some manipulations using a reformulated version of the well–known low–pass *Butterworth* filter:

$$B_{\tau,N}(x) = \left(1 + \left(\frac{x}{\tau}\right)^{2N}\right)^{-\frac{1}{2}} \tag{2}$$

$$N = rnd\left(\log_{\frac{a}{b}}\left(\frac{\beta\sqrt{1-\alpha^2}}{\alpha\sqrt{1-\beta^2}}\right)\right), \tau = a \sqrt[2N]{\frac{\alpha^2}{1-\alpha^2}} \tag{3}$$

where, $rnd(x)$ is the nearest integer value to x. The function $B(x)$ satisfies the two below conditions, $B_{\tau,N}(a) \simeq \alpha$ and $B_{\tau,N}(b) \simeq \beta$. The 2–D version of this function is defined as $B_{\tau,N}^{w,h}(x,y) = B_{w\tau,N}(x) B_{h\tau,N}(y)$, where w and h control the spread of the function in x and y directions, respectively. Assuming that the region r_i has its center on (x_i, y_i), while its height and width are w_i and h_i, respectively, we propose the function $\tilde{f}$ as:

$$\tilde{f}(x,y) = \frac{\Sigma \lambda_i B_{\tau,N}^{\frac{w_i}{2},\frac{h_i}{2}}(x - x_i, y - y_i)}{\Sigma B_{\tau,N}^{\frac{w_i}{2},\frac{h_i}{2}}(x - x_i, y - y_i)} \tag{4}$$

The function $\tilde{f}(x, y)$ proposed in (4) is a smooth version of the initial step–case function $f_\circ(x, y) = \lambda_i, [x, y]^T \in r_i$. Also, setting proper values of the parameters a, b, α, and β, the function $\tilde{f}(x, y)$ will satisfy the problem conditions. The proper set of parameters must force the corresponding kernel to be nearly one in the entire r_i, except for the borders, also preventing r_i to intrude the interior points of r_j, for $i \neq j$. Selecting a near unity (but smaller) value for a and α limits the decline of the ceil of the function, while setting $b = 1$ and a not too big value for β controls the effect of neighbor regions on each other. Setting $a = 1^-$, $\alpha = 1$, $b = 1^+$, and $\beta = 0$ is the marginal choice leading to the non–smoothed stair–case function.

As the generalization of the blockwise interpolation problem, assume the set of $m+1$–tuples $\{(r_i; \lambda_{ij})|i = 1, \cdots, n, j = 1, \cdots, m\}$, where the set of functions $f_j, j = 1, \cdots, m$ is desired to satisfy $\lambda_{ij} = \arg_\lambda \left(\forall \vec{c} \in r_i, f_j(\vec{c}) \simeq \lambda\right)$, for a set of unknown functions $f_j : R^2 \to R, j = 1, , \cdots, m$. In a similar solutions with (4), we propose:

$$\tilde{f}_j(x, y) = \frac{\Sigma \lambda_{ij} B_{\tau,N}^{\frac{w_i}{2}, \frac{h_i}{2}}(x - x_i, y - y_i)}{\Sigma B_{\tau,N}^{\frac{w_i}{2}, \frac{h_i}{2}}(x - x_i, y - y_i)} \qquad (5)$$

Here, because the set of base regions for all $\tilde{f}_j$ is the same, the total performance is increased by computing each kernel for each value of j just once. Then the problem reduces to m times computing a weighted average.

Assume that we are working in the polar coordinates. Because of the 2π discontinuity, ordinary algebraic operations on the angular variables leads to spurious results. For example $\frac{0+2\pi}{2} = \pi$, while the average of 0 radians and 2π radians equals $0 \equiv 2\pi$ radians. To overcome this problem, we propose a new method. For the given problem $\{(r_i; \theta_i)|i = 1, \cdots, n\}$ solve the problem $\{(r_i; \cos\theta_i, \sin\theta_i)|i = 1, \cdots, n\}$ to find the two functions f_{sin} and f_{cos} and then find θ using ordinary trigonometric methods. The interpolation is performed on both $\sin\theta_i$ and $\cos\theta_i$ to avoid ambiguity in the polar plane.

2.5. The Eigenimage

Assume the PCA matrix (V_r) and the expectation vector ($\vec{\eta}_r$), corresponding to the *homogenous* cluster r. For the color vector $\vec{c}$ belonging to r, $\vec{c}' = V_r^{-1}(\vec{c} - \vec{\eta}_r)$ gives the PCA coordinates. Assume that we can somehow find the color cluster $r_{\vec{c}}$ for each color vector $\vec{c}$, where $r_{\vec{c}}$ describes the *color mood* of $\vec{c}$, in the sense that, $\vec{c}' = V_{r_{\vec{c}}}^{-1}(\vec{c} - \vec{\eta}_{r_{\vec{c}}})$, satisfies, $\sigma_{c'_1} \gg \sigma_{c'_2} \gg \sigma_{c'_3}$, where $\vec{c}' = [c'_1, c'_2, c'_3]^T$. We call the images c'_1, c'_2, and c'_3 as pc_1, pc_2, and pc_3, respectively. The original image can be perfectly reconstructed using these channels, except for the numerical errors as $\vec{c}_3 = V_{r_{\vec{c}}}\vec{c}' + \vec{\eta}_{r_{\vec{c}}}$. Thus, we have $\vec{c} \simeq \vec{c}_3$. It is proved in [7] that for homogenous swatches, neglecting pc_3 or both pc_2 and pc_3 gives good approximations of the original image. Here we generalize the results for all images. Note that the perfect reconstruction does not rely on the compaction condition, while the partial reconstructions do rely on it. The partial reconstructions are $\vec{c}_2 = V_{r_{\vec{c}}}[c'_1, c'_2, 0]^T + \vec{\eta}_{r_{\vec{c}}}$ and $\vec{c}_1 = V_{r_{\vec{c}}}[c'_1, 0, 0]^T + \vec{\eta}_{r_{\vec{c}}}$. Although this scheme gives a 1–D representation of a given color image, if the computation of $V_{r_{\vec{c}}}$ and $\vec{\eta}_{r_{\vec{c}}}$ needs embedding huge information to the original image or vast computation, the scheme although being theoretically promising, but actually is not applicable. So we are seeking for a method for describing $V_{r_{\vec{c}}}$ and $\vec{\eta}_{r_{\vec{c}}}$ in a simple way. The case for defining $r_{\vec{c}} = N_{\vec{c}}$ (the neighborhood) is automatically rejected, because to compute $V_{r_{\vec{c}}}$ and $\vec{\eta}_{r_{\vec{c}}}$ we need all the neighborhood points of $\vec{c}$ leading to too much redundancy and computation cost. Also, we are not interested in computing and embedding $V_{r_{\vec{c}}}$ and $\vec{\eta}_{r_{\vec{c}}}$ to each pixel, which leads to 1100% redundancy. Here, we propose a fast method for computing corresponding $V_{r_{\vec{c}}}$ and $\vec{\eta}_{r_{\vec{c}}}$ for all the pixels. Assume feeding the given image I to the bi–tree (or equivalently to the quad–tree) decomposition method. The output of the decomposition method is the matrix Λ containing the coordinates of r_i along with the expectation matrix $\vec{\eta}_i$ and the polarized version of the PCA matrix $(\theta_i, \phi_i, \psi_i)$. Storing this portion of the Λ matrix needs $10n$ bytes. For ordinary values of n abour 200 in a 512×512 image, Λ will take about $\frac{1}{4000}$ of the original image. Now assume solving the problem $\{(r_i; \xi_i)|i = 1, \cdots, n\}$ using the blockwise interpolation, where ξ_i is the row vector containing η_{i_1}, η_{i_2}, η_{i_3}, θ_i, ϕ_i, and ψ_i. Note that, the three values of θ_i, ϕ_i, and ψ_i are angular values. Assume the solutions of the problem as the functions $\tilde{\eta}_1$, $\tilde{\eta}_2$, $\tilde{\eta}_3$, $\tilde{\theta}$, $\tilde{\phi}$, and $\tilde{\psi}$. Now we compute the functions $\tilde{\vec{\eta}} : R^2 \to R^3$ and $\tilde{V} : R^2 \to R^9$, as the value of the expectation vector and the PCA matrix in each pixel, respectively. Using the PCA projection, the three *eigenimages* pc_1, pc_2 and pc_3 are computed as $[pc_1(x, y), pc_2(x, y), pc_3(x, y)]^T = \tilde{V}(x, y)^{-1}[I(x, y) - \tilde{\vec{\eta}}(x, y)]$. We call the function $\tilde{\vec{\eta}} : R^2 \to R^3$ as the *expectation map* (Emap) and the polarized version of $\tilde{V} : R^2 \to R^9$ as the rotation map (Rmap), respectively. As the PCA theory states [10], we expect the standard deviation of the three planes to be descending, with σ_{pc_1} more larger than others. From linear algebra we have that for orthonormal transformation V_r we have, $\sigma_{pc_1}^2 + \sigma_{pc_2}^2 + \sigma_{pc_3}^2 = \sigma_r^2 + \sigma_g^2 + \sigma_b^2$. Thus, $\kappa_i = \sigma_{pc_1}^2/(\sigma_{pc_1}^2 + \sigma_{pc_2}^2 + \sigma_{pc_3}^2)$ gives the amount of information available in the i–th eigenimage. Note that $\kappa_1 + \kappa_2 + \kappa_3 = 1$.

2.6. Proposed Watermarking Method

Assume the image I with the three eigenimages pc_1, pc_2, and pc_3. Although, there is no orthogonality constraint in the eigenimage theory, but the eigenimage approach can be adapted for watermarking purposes. Assume that the gray–

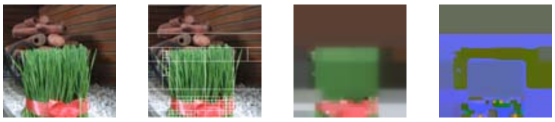
(a) (b) (c) (d)

Fig. 1. (a) Original Image (adopted from [11]). (b) Result of Bi-tree decomposition. (c) Emap. (d) Rmap.

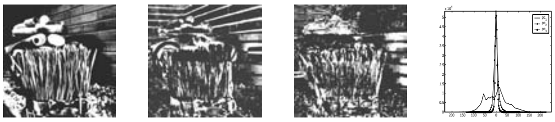
pc_1 pc_2 pc_3

Fig. 2. Eigenimages of the sample image and their histogram.

scale image W is to be embedded into I as a watermark. Also, assume that I and W are of the same size. First the dynamic range of W is fit into pc_3 domain, as $\tilde{W} = \tilde{\sigma}_{pc_3}(W - \eta_W)/\sigma_W$. Replacing the pc_3 with the scaled version of the watermark ($\tilde{W}$), the watermarked image is reconstructed (I'). The process of extracting the watermark is vice versa: compute the eigenimages corresponding to the given image as pc'_1, pc'_2, and pc'_3. Clearly pc'_3, when normalized, contains the watermark. We propose the normalization scheme as $W' = 255/(2\sigma_{pc'_3})(pc'_3 - \eta_{pc'_3} - \sigma_{pc'_3})$.

3. EXPERIMENTAL RESULTS

The proposed algorithms are developed in *MATLAB 6.5*, on an *1100 MHz Pentium III* personal computer with $256MB$ of *RAM*.

Assume the image shown in figure 1-a, which is decomposed with parameters of $p = 0.5$, $\varepsilon_1 = 5$, and $\varrho = 5$ into 91 blocks (see figure 1-b). Figures 1-c and 1-d show the corresponding EMap and RMap, and figure 2 shows the three pc_i channels. Note that the dynamic range is exaggerated in all eigenimages to give a better visualization. The stochastic distribution of pc_i is investigated in figure 2–d which shows the histogram of the three eigenimages corresponding to the image shown in figure 1-a. In this example the standard deviations of the pc planes are computed as: $\sigma_{pc_1} = 52$, $\sigma_{pc_2} = 12$, and $\sigma_{pc_3} = 6$, leading to $\kappa_1 = 94\%$, $\kappa_2 = 5\%$, and $\kappa_3 = 1\%$.

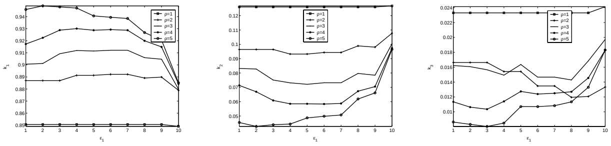
(a) (b) (c)

Fig. 3. The energy distribution of the eigenimages for different values of ε_1 and ϱ. (a)κ_{pc_1}, (b)κ_{pc_2}, (c)κ_{pc_3}.

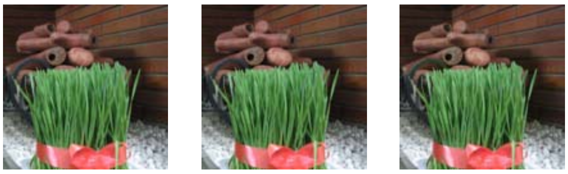
(a) (b) (c)

Fig. 4. Results of reconstructing the sample image from its eigenimages, (a) using all eigenimages ($PSNR = 60dB$), (b) ignoring one eigenimage ($PSNR = 38dB$), and (c) ignoring two eigenimages ($PSNR = 31dB$).

Figure 3-a, 3-b, and 3-c show the values of κ_1, κ_2, and κ_3 for the image in figure 1-a for different values of ε_1 and ϱ. Rather than the trivial cases of $\varrho \leq 2$ and $\varepsilon_1 > 9$ (which are never actually used) more than 90% of the image energy is compacted in pc_1, while pc_2 and pc_3 hold about 9% and 1% of the energy, respectively. Having in mind that $\kappa_r = 38\%$, $\kappa_g = 32\%$, and $\kappa_b = 30\%$ in the original image, the energy compaction of the proposed eigenimage extraction method is clear.

Figure 4 shows the results of reconstructing the sample image from its corresponding eigenimages. While figure 4-a shows the result of reconstructing the image using all three eigenimages, figures 4-b and 4-c show the results of ignoring pc_3 and both pc_3 and pc_2, respectively. The resulting $PSNR$ values are $60dB$, $38dB$, and $31dB$. Note that $PSNR = 60dB < \infty$ when reconstructing the image using all eigenimages is caused only by numerical errors, while the two other $PSNR$ values ($38dB$ and $31dB$) shows the loss of information. Figure 5 shows the $PSNR$ values obtained by reconstructing the image using all the three channels (figure 5-a), only two channels (figure 5-b), and just one channel (figure 5-c), for different values of ε_1 and ϱ. For values of $\varepsilon_1 \leq 8$ and $\varrho \geq 3$, reconstructing the image using all eigenimages gives the high $PSNR$ value of about $60dB$, while neglecting one and two eigenimages, results in $PSNR \geq 35dB$ and $PSNR \geq 28dB$.

Figure 6-b shows the results of embedding the watermark shown in Figure 6-a into the image shown in figure 1-

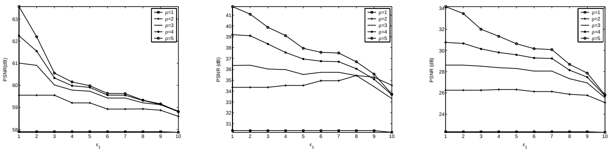
(a) (b) (c)

Fig. 5. $PSNR$ values of image reconstruction using (a) three eigenimages, (b) two eigenimages, and (c) one eigenimage for different values of ε_1 and ϱ.

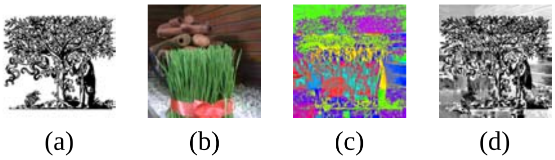
(a) (b) (c) (d)

Fig. 6. Results of the proposed watermarking method performed on the sample image. (a) Watermark signal. (b) Watermarked image with $PSNR = 35dB$. (c) Exaggerated difference between the original image and the watermarked image. (d) Extracted watermark.

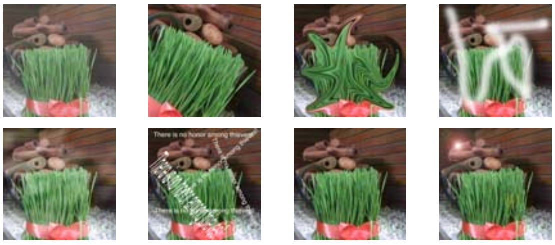

Fig. 7. The attacked watermarked images.

a with the resulting $PSNR$ equal to $35dB$. Figure 6-c shows the exaggerated difference between the original image and the watermarked image, and Figure 6-d shows the extracted watermark. Investigating figure 6-c shows where the method hides the data; at each pixel, the direction of the third principal component shows the direction in which data can be placed while not affecting the visual appeal of the image.

To test the robustness of the proposed watermarking method against invasive attacks, 42 sample images containing *Lena*, *Mandrill*, *Girl*, *Couple*, *Airplane*, and *Peppers* and 9 watermarks of the logos of *Sharif University of Technology*, *IEEE*, and *Elsevier* is investigated. The watermarked images are attacked by some methods using the *Adobe Photoshop 6.0*. Figure 7 shows some of the attacked watermarked images and figure 8 shows the corresponding extracted watermarks.

Investigating figure 8 along with other numerous tests shows that the proposed watermarking method is robust against linear and nonlinear geometrical transformations including rotation, scaling, cropping, and other geometrical distortions. Also, it is robust against occlusion, artistic effects, captioning, noise addition, enhancement operations like brightening and increasing contrast (even when performed locally), lossy compression, frequency domain filtering, and different kinds of blurring.

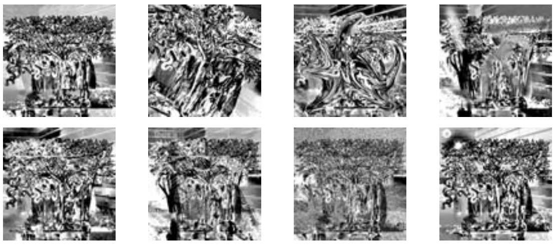

Fig. 8. The extracted watermarks.

Table 1 compares the proposed watermarking method with the best methods available in the literature. The table lists the watermark capacity of each method when embedding to a 512×512 color image along with the domain in which data is embedded. Also, the attack resistance of different approaches is compared here. It is observed in different experiments that the standard deviation of pc_3 in a typical image is more than 4. Thus, using the proposed watermarking method on a 512×512 color image at least a same–sized $2bpp$ image can be used as the watermark signal. This makes the watermark capacity of the proposed method equal to 64KB. This is four times more than the highest capacity of the available approaches (the method by *Barni et. al.* [12]). The only approaches using the color vectors are proposed by *Chou et. al.* [6] and *Piyu et. al.* [4]. Note that, the method by *Chou et. al.* [6] is the only method showing resistance to the linear point operations like brightening and contrast enhancement. It must be emphasized that their method's resistance is limited to the global such operations, while our proposed method is resistant even to local linear point operations (see Figure 7–f,g). Unfortunately, no attention is spent on non–linear geometrical operations like elastic and perspective transformation and image editing processes like adding text, artistic effects, occlusion and so on. While many copyrighted images are used in books, posters, and websites where they appear with some levels of artistic manipulation, the non–efficiency of the available watermarking literature in dealing with these attacks is a real shortcoming. Table 1 depicts that the proposed method is the only available method resistant to the seven groups of attacks listed in its caption.

4. CONCLUSIONS

A new PCA–based watermarking method is proposed that uses the spectral redundancy in an image to embed a same–sized gray–scale image into it. The experimental results show that, while the method gives high values of $PSNR$ and no subjective artifact, it is highly resistant against invasive attacks. The method responds promisingly when dealing with attacks in the spatial domain (linear and non–linear geometrical transformations), the spectral domain (manipulating the contrast, brightness both globally and locally), and frequency domain (filtering and blurring). To the best knowledge of the authors no watermarking method with such robustness is available in the

Table 1. Comparison of different watermarking methods with the proposed method used in a 512×512 image. –: Not Resistant. $\sim$: Partially Resistant. $\surd$: Completely Resistant. [Abbreviations: G: Grayscale, SCC: Single Color Component, CV: Color Vector, LG: Linear Geometrical Transformation, NLG: Nonlinear Geometrical Transformation, LPO: Linear Point Operations, NLPO:Nonlinear Point Operations, SO: Spatial Domain Operations, EO: Editing Operations, CMP: JPEG Compression]

Method		[13]	[14]	[15]	[6]	[3]	[12]	[16]	[17]	[18]	[19]	[4]	Proposed
Capacity		4KB	8KB	8KB	2KB	1KB	16KB	8B	0.5KB	60B	64B	2KB	64KB
Domain		G	G	G	CV	SCC	SCC	SCC	G	G	G	CV	CV
Res.	LG	∼	√	∼	∼	∼	√	–	√	√	∼	∼	√
	NLG	–	–	–	–	–	–	–	–	–	–	–	√
	LPO	–	–	–	∼	–	–	–	–	–	–	–	√
	NLPO	–	∼	∼	∼	∼	∼	–	∼	–	–	∼	√
	SO	–	∼	∼	∼	∼	∼	–	∼	∼	∼	∼	√
	EO	–	–	–	–	–	–	–	–	–	–	–	√
	CMP	√	√	√	√	√	√	∼	√	√	√	√	√

Acknowledgement

The first author wishes to thank Ms. *Azadeh Yadollahi* for her encouragement and invaluable ideas.

5. REFERENCES

[1] M.D. Swanson, M. Kobayashi, and A.H. Tewfik, “Multimedia data–embedding and watermarking technologies,” *IEEE*, vol. 86(6), pp. 1064–1087, June 1998.

[2] M. Kutter, F. Jordan, and F. Bossen, “Digital watermarking of color images using amplitude modulation,” *Electronic Imaging*, vol. 7(2), pp. 326–332, April 1998.

[3] Pao-Ta Yu, Hung-Hsu Tasi, and Juh-Shyan Lin, “Digital watermarking based on neural networks for color images,” *Signal Processing*, vol. 81, pp. 663–671, 2001.

[4] Piyu Tsai, Yu-Chen Hu, and Chin-Chen Chang, “A color image watermarking scheme based on color quantization,” *Signal Processing*, vol. 84, pp. 95–106, 2004.

[5] S.A.M. Gilani, I. Kostopoulos, and A.N. Skodras, “Color image–adaptive watermarking,” in *14th Int. Conf. on Digital Signal Processing(DSP2002)*, Santorini, Greece, 1–3 July 2002, vol. 2, pp. 721–724.

[6] Chun-Hsien Chou and Tung-Lin Wu, “Embedding color watermarks in color images,” *EURASIP Journal on Applied Signal Processing*, vol. 1, pp. 327–332, 2001.

[7] Arash Abadpour and Shohreh Kasaei, “A new parametric linear adaptive color space and its pca–based implementation,” in *The 9th Annual CSI Computer Conference, CSICC*, Tehran, Iran, Feb. 2004, pp. 125–132.

[8] Arash Abadpour and Shohreh Kasaei, “Performance analysis of three homogeneity criteria for color image processing,” in *IPM Workshop on Computer Vision*, Tehran, Iran, 2004.

[9] H. Samet, “Region representation: Quadtrees from boundary codes,” *Comm. ACM*, vol. 21, pp. 163:170, March 1980.

[10] H. Hotteling, “Analysis of a complex of statistical variables into principal components.,” *Journal of Educational Psychology*, vol. 24, pp. 417–441, 1933.

[11] Shohreh Tabatabaii Seifi and Ali Qanavati, “Digital color image archive,” Qnavati@mehr.sharif.edu.

[12] Mauro Barni, Franco Bartolini, and Alessandro Piva, “Multichannel watermarking of color images,” *IEEE Transaction on Circuits and Systems for Video Technology*, vol. 12(3), pp. 142–156, 2002.

[13] J.J.K. Ruanaidh, W.J. Dowling, and F.M. Boland, “Watermarking digital images for copyright protection,” *IEE Proceedings on Vision, Signal and Image Processing*, vol. 143(4), pp. 250–256, August 1996.

[14] Athanasios Nikoladis and Ioannis Pitas, “Robust watermarking of facial images based on salient geometric pattern matching,” *IEEE Transaction on Multimedia*, vol. 2(3), pp. 172–184, September 2000.

[15] Ming-Shing Hsieh, Din-Chang Tseng, and Yong-Huai Huang, “Hiding digital watermarks using miltiresolution wavelet transform,” *IEEE Transaction on Industrial Electronics*, vol. 48(5), pp. 875–882, October 2001.

[16] Martin Kutter and Stefan Winkler, “A vision–based masking model for spread–spctrum image watermarking,” *IEEE Transaction on Image PRocessing*, vol. 11(1), pp. 16–25, January 2002.

[17] Chih-Wei Tang and Hsueh00Ming Hang, “A feature–based robust digital image watermarking scheme,” *IEEE Transaction on Signal Processing*, vol. 51(4), pp. 950–959, April 2003.

[18] Xiangui Kang, Jiwu Huang, Yun Q. Shi, and Yan Lin, “A dwt–dft composite watermarking scheme robust to both affine transform and jpeg compression,” *IEEE Transactions on Circuits and Systems for Video Technology*, vol. 13(8), pp. 776–786, August 2003.

[19] Shih-Hao and Yuan-Pei Lin, “Wavelet tree quantization for copyright protection watermarking,” *IEEE Transactions on Image Processing*, vol. 13(2), pp. 154–165, February 2004.